Growth and melting of droplets in cold vapors

Jean-Marc L'Hermite
Laboratoire Collisions, Agrégats Réactivité, IRSAMC, UPS–Université de Toulouse–CNRS UMR 5589, 31062 Toulouse, France
(Received 19 June 2009; revised manuscript received 8 October 2009; published 13 November 2009)

A model has been developed to investigate the growth of droplets in a supersaturated cold vapor taking into account their possible solid-liquid phase transition. It is shown that the solid-liquid phase transition is nontrivially coupled, through the energy released in attachment, to the nucleation process. The model is based on the one developed by J. Feder, K. C. Russell, J. Lothe, and G. M. Pound [Adv. Phys. **15**, 111 (1966)], where the nucleation process is described as a thermal diffusion motion in a two-dimensional field of force given by the derivatives of a free-energy surface. The additional dimension accounts for droplets internal energy. The solid-liquid phase transition is introduced through a bimodal internal energy distribution in a Gaussian approximation derived from small clusters physics. The coupling between nucleation and melting results in specific nonequilibrium thermodynamical properties, exemplified in the case of water droplets. Analyzing the free-energy landscapes gives an insight into the nucleation dynamics. This landscape can be complex but generally exhibits two paths: the first one can generally be ascribed to the solid state, while the other to the liquid state. Especially at high supersaturation, the growth in the liquid state is often favored, which is not unexpected since in a supersaturated vapor the droplets can stand higher internal energy than at equilibrium. From a given critical temperature that is noticeably lower than the bulk melting temperature, nucleation may end in very large liquid droplets. These features can be qualitatively generalized to systems other than water.

DOI: 10.1103/PhysRevE.80.051602 PACS number(s): 82.60.Nh, 64.70.D−, 64.60.an

I. INTRODUCTION

The formation of droplets in supersaturated vapors has attracted considerable attention for a century [1]. The condensation of a vapor into liquid or solid phase occurs through the formation of droplets that continuously grow from the monomers of the vapor [2–4]. The growth of droplets by successive attachment of monomers is called nucleation, which is homogeneous when no pre-existing seeds exist. Many nucleation theories have been developed with the aim of describing this growth that occurs in the so-called supersaturated vapors whose pressure is higher than the equilibrium vapor pressure over liquid (or solid) phase. Although a lot of theoretical effort has been devoted to this topic [4], no reliable accurate quantitative theory of this phenomenon has been proposed up to now. A large majority of the nucleation models are derived from the so-called classical nucleation theory (CNT) of Becker and Döring [2]. These models rest on the following common basis [3,4]. A particular growing regime is ensured, characterized by a constant flux of growing droplets independent of their size. This regime is established after a brief transient regime, in which the number of larger and larger droplets increases roughly exponentially. The duration of this transient regime is negligible for gas nucleation [5]. The purpose of nucleation theories is to predict nucleation rates, defined as the number of droplets formed per unit time and unit volume in the vapor. In the constant flux regime, the nucleation rate does not depend on the size, provided it is large enough [3,4]. Unfortunately, calculations still fail to predict the observed nucleation rates, often by orders of magnitude, suggesting failures in nucleation theories (for a review of these deficiencies, see, for instance, [6]). A well-identified problem is the lack of reliable data and theories for describing the evolution of the physical properties of the droplets over the huge size range from the monomer to visible droplets: nucleation theories must deal simultaneously with molecular and mesoscopic scales. Another major issue is related to the thermalization of the droplets between successive collisions, which is not taken into account in CNT. The thermodynamic phase of the droplets is also expected to affect their growth. As will be discussed below, no specific theoretical study has been devoted to this issue.

The present work addresses an issue that has never been considered so far, to our knowledge, namely, the effect of melting on the nucleation process. The melting properties of small droplets are particular: both melting temperature and molecular latent heat of melting decrease with the size in most cases [7]. The main purpose of the model presented in this paper is to address the following issue: what happens during the growth of droplets when the temperature of the vapor is higher than the melting temperature of very small droplets, but lower than the bulk melting temperature? These two conditions are often fulfilled over a wide temperature range, of almost 100 K for water. The present work puts together a nucleation model that can able to deal with cluster internal energy (such a model is called nonisothermal) and a capillary model for describing the melting transition of small droplets. In Sec. II, classical and nonisothermal nucleation models are presented and the need for introducing melting in nucleation theory is demonstrated. Our nucleation model, in which the solid or the liquid nature of the growing droplets is taken into account, is presented in Sec. III, and finally the results obtained for water droplets are described in Sec. IV.

II. NUCLEATION AND MELTING

A. Classical isothermal nucleation theories

The properties at the mesoscopic scale are generally described in the framework of the so-called capillarity approximation [3,4], which essentially relies on the increase in the surface to volume ratio as the size decreases. Some of these "small-size effects" have been known for centuries: as far

back as in the early 18th century, Laplace already calculated the energy penalty introduced by the curvature of a small droplet, which is a typical capillary effect. The basic idea of capillarity physics is that the binding energy of surface atoms (or molecules) is lower than the one of inner atoms since they have fewer bonds. At a given temperature, these more loosely bound atoms are more likely to evaporate than in the volume: in small droplets there are many loosely bound surface atoms; thus, the equilibrium vapor pressure is higher than in the bulk. Consequently, a vapor pressure higher than the bulk equilibrium vapor pressure can be lower than the equilibrium vapor pressure of small droplets. The supersaturation S is defined as the ratio of the actual pressure to the bulk equilibrium vapor pressure over the liquid (or solid) phase. For $S>1$ there is a size for which the evaporation rate exactly compensates the collision rate, which is thus at equilibrium with the vapor. Above this critical size, the vapor can be really considered as oversaturated and the growth proceeds very rapidly since the sticking rate is higher than the evaporation rate. On the other hand, for droplets smaller than this critical size, the evaporation rate is higher than the attachment rate, and the growth is possible only owing to favorable fluctuations of the decay time, which is closely related to the statistical fluctuations of internal energy.

The basic idea of nucleation theory is that the nucleation rate is determined by the probability for reaching the critical size, which bottlenecks the flux. The free energy at the critical size can be considered as an activation barrier. This assumption is rather simple but its application comes up against huge practical difficulties. One of the problems is that the properties of very small droplets, which are generally unknown, may strongly depart from the approximations used at the mesoscopic scale. For instance, the concept of surface tension accounts nicely for the smooth variations with the size of the surface energy of large droplets, but it is less relevant for clusters of tens or hundreds of molecules. In this regime, the dissociation energy may vary in a nonmonotonous way [8]. Quantum effects on the nucleation of small clusters have been studied [9]. Nucleation models try to deal with the disagreement between theory and experiments through empirical [10] or phenomenological [11] corrections. Some models are in satisfactory agreement with experiment but at the cost of a number of adjustable parameters [12]. The effect of internal [13,14] or external (translational) [3,15] degrees of freedom and the failures of CNT at very small sizes [3,9,16–18] have already been analyzed.

B. Nonisothermal nucleation theories

It is not our purpose to enumerate here all the deficiencies of nucleation theories, and we will now focus on a particular issue related to the internal energy of the droplets. In most studies, the temperatures of the droplets and the vapor are assumed to be the same. This assumption requires that, after a sticking collision, the cluster is thermalized before it undergoes the next collision. In pure homogeneous nucleation without any buffer vapor, this is wrong: a sticking collision increases the internal energy of the droplet by the binding energy of a monomer plus the collision energy. The effect of this heat of association is to create short-lived states that will decay before undergoing thermal equilibrium by collisions with single vapor molecules [19]. Note that radiative cooling is negligible on the time scale of molecular collisions in a vapor [20,21]. With a sufficiently high pressure of carrier gas this effect could be expected to vanish since the frequent collisions with the carrier gas are likely to keep permanently the clusters at the temperature of the vapor. The effects of carrier gas pressure and of heat of association have been addressed experimentally [22,23] and theoretically [24–27], but with contradictory conclusions. It is worth noting that in nucleation experiments the relative density of the buffer gas is seldom greater than several hundreds (see, for instance, Ref. [28] in the case of water nucleation), whereas experiments involving thermalization of sodium clusters in a heat bath have shown that the number of collisions required to thermalize efficiently small droplets is at least on the order of 10^4 [29,30]; thus, in many experiments, droplets are unlikely to be thermalized at the temperature of the vapor. That the temperatures of nucleating droplets and their surrounding differ from each other had already been mentioned in early papers [31,32]. Nevertheless, most CNT theories cannot deal with this issue since the droplets and the vapor are assumed to be at the same temperature, whereas the internal energy of the droplets should be treated as a free parameter and explicitly included in the rate equations. This issue is addressed in the so-called nonisothermal nucleation studies, using molecular-dynamics [25] or stochastic [33] simulations, by numerically solving the coupled mass and energy balance equations [34–36] or by finding approximate analytical solution of these equations [1].

Although the different predictions of these studies do not always match, some common conclusions emerge. First, beyond the critical size the droplets are warmer than the surrounding vapor, which is not surprising since in this case the attachment rate is higher than the evaporation rate, allowing droplets to stand a higher decay rate and thus a higher internal energy than at equilibrium. For subcritical clusters, most studies show that the droplets are colder than the vapor, which is again in accordance with intuition since in this size range droplets grow through favorable statistical fluctuations of their decay rate that is reduced at low internal energy. As emphasized by Barrett *et al.* [34], there is often confusion between energy and temperature in the literature; one must take care of nucleation being a *nonequilibrium* phenomenon for which the temperature is not necessarily the most relevant parameter: the internal energy distribution of growing droplets is not the one of the canonical ensemble.

C. Melting and nucleation

A very simple question has not been addressed so far in nucleation models: are the droplets liquid or solid? Experimental works have strongly suggested that, even in vapors at a temperature far below the bulk melting temperature, droplets are likely to grow in the liquid state before subsequently mature to ice particles [37]. What is the effect of the melting transition on the nucleation process and conversely how does nucleation modify the melting? The present paper incorpo-

rates the melting transition in nucleation theory. We do not deal here with the freezing nucleation as addressed in nucleation models close to the gas nucleation theory [4,38–40] or in the frame of transport theory [41]. In these studies the temperature is well defined and particles do not grow. The freezing transition has also been investigated experimentally in the case of water [42,43]. Our goal here is not to describe the freezing of droplets of fixed size in thermodynamic equilibrium with a gaseous environment, but the possible transition from liquid to solid or from solid to liquid of droplets during their growth, where nucleation and melting are coupled in the out of equilibrium constant flux regime considered in gas nucleation theories.

The interplay between nucleation and melting transition is complex for two reasons: first the melting temperature of a droplet depends on its size and second the internal energy distribution of the droplets is significantly modified by the nucleation process, as shown in nonisothermal nucleation theories. Our model is based on the approach of Feder *et al.* [1], which still remains a landmark work and is particularly tractable for our purpose. Feder and co-workers showed that nucleation can be reduced to a diffusion process in a two-dimensional space using a particular system of coordinates. The first coordinate is close to the size of the droplets and the second is close to their internal energy. Diffusion takes place in a field of force defined by the gradient of a free-energy surface. In Feder's study, melting is not introduced and this surface is rather simple, so that nucleation rates can be approximated analytically. Introducing melting leads to more complex surfaces and finding an analytical expression of nucleation rates is no longer possible. Providing accurate predictions is out of reach of the present study, which aims at disclosing qualitatively the features introduced by the interplay between nucleation and melting. Nevertheless, merely analyzing the shape of the free-energy landscape and using qualitative arguments offer a good insight into the growth dynamics of droplets that can freeze or melt. The model is exemplified in the case of water.

III. NUCLEATION MODEL FOR MELTING AND FREEZING DROPLETS

We first recall in Sec. III A the essentials of the melting of small particles and how they are accounted for here in the case of water. Section III B is a review of Feder's theory of nucleation. In Sec. III C, one shows how the melting transition of the droplets is inserted in nucleation theory.

A. Melting of small particles

The melting of small particles is not yet fully understood [7]. Recent experimental investigations on small clusters of tens to hundreds of atoms have shown that the size dependence of both the melting temperature and the latent heat of fusion can be strongly nonmonotonous [44–46]. For intermediate-size particles, i.e., in the capillarity regime, the size evolution of melting temperatures and enthalpies of fusion is also poorly documented [7]. It is generally suggested that both melting temperature and latent heat of fusion decrease with the size of the particle, following approximately a $1/r$ law, where r is the radius of the particle [7,30]. The transition from the nonmonotonous behavior at very small size to a smooth $1/r$ law is documented only for sodium clusters [47]: for sufficiently large clusters (from sizes of about 200 for sodium), the scaling of melting temperature with the size n seems to converge toward the capillarity approximation. The size dependence of the melting temperature at intermediate size has been experimentally characterized for gold [48] and tin [49] droplets. The variation of the enthalpy of fusion has also been estimated for tin [49] and water [50]. These experimental investigations, carried out for particles deposited on a surface, confirm approximately the $1/r$ variation of melting temperature and latent heat of fusion. Although for most compounds (including water) there is no experimental evidence for this behavior, we will consider that the melting temperature of droplets follows the regular $1/r$ (or equivalently $n^{-1/3}$, where n is the number of molecules in the cluster) law,

$$T_{melt}(n) = T_{melt}(\text{bulk}) - \alpha n^{-1/3}. \quad (1)$$

It will also be assumed that the latent heat of fusion follows a similar law [7],

$$L_{melt}(n) = L_{melt}(\text{bulk}) - \beta n^{-1/3}. \quad (2)$$

For water, α can be estimated from the differential scanning calorimetry experiment described in Ref. [50] and simulations on small clusters [51]. Although it has not been demonstrated that in the case of water there is a smooth transition from intermediate size to very small clusters, one can find a value of $\alpha = 3 \times 10^2$, consistent with both references. Using this value, $T_{melt}(100) = 208$ K. The latent heat of fusion in the temperature range studied here can be estimated from the value used by Ford in a study of the freezing nucleation of ice clusters [40] and from the simulations by Douady *et al.* at small sizes [51]. The values used here are $L_{melt}(\text{bulk}) = 0.045$ eV/molecule and $\beta = 10^2$. With these values, $L_{melt}(100) = 0.023$ eV/molecule.

As will be shown in the following, a model of droplet internal energy distribution in the canonical ensemble is also required. In conventional nonisothermal nucleation theories, this internal energy distribution is often approximated by a Gaussian function that accounts for intrinsic statistical fluctuations [1]. Barrett *et al.* showed that this Gaussian approximation does not introduce significant errors in nonisothermal nucleation models [34]. Previous nonisothermal nucleation models usually represent the internal energy distribution by a single Gaussian [1]. When the solid-liquid phase transition is taken into account, this distribution is split into two Gaussian components. This kind of bimodal energy distribution at the phase transition is now well established for finite-size systems such as clusters. It has been confirmed experimentally for sodium clusters [52]. Bimodal energy distributions near a phase transition are also found in a variety of systems of finite size or interacting via long-range forces [53]. The internal energy distribution of a cluster in the canonical ensemble is well accounted for by the superposition of two Gaussians, as illustrated in Fig. 1, the first one corresponding to the solid state and the other to the liquid state, each with a

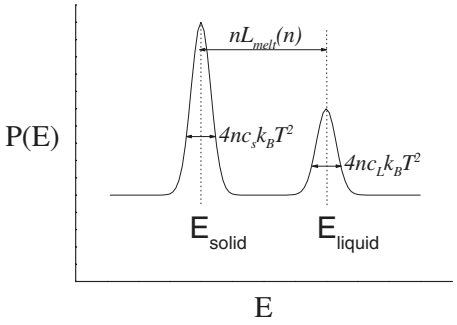

FIG. 1. Gaussian representation of cluster internal energy distribution just below the melting transition.

finite width from intrinsic fluctuations [54–56]. The gap between the centers of the two Gaussians is the total latent heat of melting $nL_{melt}(n)$.

In finite systems, the solid-liquid transition occurs over a temperature range $\Delta T = k_B T_{melt}^2/(nL)$ (k_B is the Boltzmann constant; the size dependence of L is implicit here and in the following) [57]. The relative weight of solid and liquid droplets (i.e., the relative area of the two peaks in Fig. 1) varies smoothly over this width around the melting temperature. This can be accounted for by weighting the solid and the liquid by the functions θ_S and θ_L, which are normalized factors proportional to the surface of the solid and the liquid peaks, respectively. θ_S and θ_L are given by

$$\theta_S(T) = \frac{1}{1+\exp[(T-T_m)/(\Delta T/2)]}, \quad \theta_l(T) = 1 - \theta_S(T). \tag{3}$$

These weighting functions have been successfully used in simulations of experimental caloric curves of small clusters [58]. The normalized internal energy distribution is finally written as

$$F(T,n,\varepsilon) = (2\pi n c_l k_B T^2)^{-1/2}[\theta_S(T)\exp(-\varepsilon_s^2/2nc_S k_B T^2) + \theta_l(T)\exp(-\varepsilon_l^2/2nc_l k_B T^2)] \tag{4}$$

with $\varepsilon_S = \varepsilon$ and $\varepsilon_L = \varepsilon - nL$.

The first term is a normalization factor. ε, called the energy fluctuation [1,34], is the difference between the actual internal energy and the mean internal energy that the droplet would have in the canonical ensemble at the temperature T. c_S and c_l are the molecular heat capacities of the solid and the liquid, respectively. They are considered equal here.

B. Feder's diffusion approach to nucleation

In all classical isothermal approaches, the nucleation rate J_{ISO} is obtained in the form [1–4]

$$J_{ISO} = AZ\exp[-\Delta G^0(n^*)/k_B T]. \tag{5}$$

Here, $\Delta G^0(n^*)$ is the free energy of formation of the critical cluster of size n^* for which the evaporation rate exactly compensates the attachment rate. A is a kinetic factor whose exact expression slightly varies from one model to another. Z is the so-called Zeldovich factor, related to the curvature of the free energy at the critical size $\Delta G^0(n^*)$ [3,4],

$$Z = \left[-\frac{1}{2\pi}\left(\frac{\partial^2 \ln c_0(n^*)}{\partial n^2}\right)\right]^{1/2}. \tag{6}$$

Z is obtained in a parabolic approximation of $\Delta G^0(n)$ near n^*, where by definition the n-partial first derivative of $\Delta G^0(n)$ vanishes. The Zeldovich factor can be understood as accounting for the mean time required to overcome the free-energy barrier around the critical size within an energy range $k_B T$ [1].

Classical isothermal nucleation theories are one dimensional insofar as the growth is described as a function of the single variable n. In the 1960s, Feder and co-workers proposed a two-dimensional treatment that allows dealing simultaneously with size and internal energy [1]. We recall here the backgrounds of this model. The equations of the original paper are not extensively developed here but one rather emphasizes the physical bases on which the model relies. It is important to ensure that introducing the melting transition does not invalidate the assumptions of the initial model. Some particular points are detailed for this purpose.

In Feder's theory, the nucleation rate is the constant flux solution of the system of two-dimensional coupled rate equations,

$$\frac{\partial c(n,\varepsilon,t)}{\partial t} = \int_{-\infty}^{+\infty} d\varepsilon' \int_1^{\infty} dn' \{c(n',\varepsilon',t)R\langle n,\varepsilon|n',\varepsilon'\rangle - c(n,\varepsilon,t)R\langle n',\varepsilon'|n,\varepsilon\rangle\}, \tag{7}$$

where $c(n,\varepsilon,t)$ is the population of clusters of size n and fluctuation energy ε ($\varepsilon=0$ in isothermal theories). $R\langle n,\varepsilon|n',\varepsilon'\rangle$ and $R\langle n',\varepsilon'|n,\varepsilon\rangle$ are shorthand notations for the probabilities to reach n,ε from n',ε' and n',ε' from n,ε, respectively. The first term in the left member accounts for the positive contribution to the population of clusters of size n due to either growth from sizes $n'<n$ or evaporation from sizes $n'>n$. The second term represents the losses at size n due to either evaporation or sticking of clusters of size n. It is assumed, as usual, that growth and decay of single molecules greatly predominate over attachment or evaporation of clusters, then the integration over n' is restricted to $n\pm 1$. Within this restriction, Eq. (7) reads

$$\frac{\partial c(n,\varepsilon,t)}{\partial t} = \int_{-\infty}^{+\infty} d\varepsilon' \{c(n-1,\varepsilon',t)R_c\langle n,\varepsilon|n-1,\varepsilon'\rangle + c(n+1,\varepsilon',t)R_v\langle n,\varepsilon|n+1,\varepsilon'\rangle\} - \int_{-\infty}^{+\infty} d\varepsilon' c(n,\varepsilon,t)\{R_c\langle n+1,\varepsilon'|n,\varepsilon\rangle + R_v\langle n-1,\varepsilon'|n,\varepsilon\rangle\}. \tag{8}$$

R_c and R_v stand for attachment rates and evaporation rates, respectively. All classical nucleation models can be derived from rate equations such as Eq. (7) [3,4], but without the integration over ε' in isothermal theories. Introducing ε allows taking into account the energy brought to a droplet at each sticking. The mean internal energy added in attachment is

$$q = h - \frac{k_B T}{2} - \sigma\, \partial A(n)/\partial n, \tag{9}$$

where h is the molecular latent heat of evaporation, σ is the surface tension, and $A(n)$ is the surface of a droplet of size n. The second term $k_B T/2$, which essentially accounts for the mean relative translational energy of the cluster and the molecule, is controversial [13,34] but affects the final results in a negligible way [34]. This term is generally very small with respect to the latent heat of evaporation h (in the case of water, for example, h is on the order of 0.5 eV, whereas $k_B T/2$ is on the order of 0.01 eV at 250 K). The intrinsic energy fluctuations of the impinging molecules are introduced in a Gaussian approximation by adding to q a stochastic energy x, whose statistical distribution is obtained from the fluctuation-dissipation relation $c_V \approx 1/k_B T^2\ \mathrm{var}(x)$, where c_V is the heat capacity of the vapor and $\mathrm{var}(x)$ is the variance of the variable x. The internal energy of a cluster is eventually increased upon a sticking collision by $(q+x)$.

The condensation terms R_c are approximated assuming geometrical cross sections (i.e., within the hard sphere model). The impingement frequency of a single molecule onto a cluster of size n is $\beta(T,x)A(n)$, where $A(n) = (36\pi)^{1/3} v_m^{2/3} n^{2/3}$ (v_m is the molecular volume) is the surface of the droplet [4]. The attachment cross sections of small particles may be enhanced with respect to the hard sphere approximation due to long-range interaction (it is indeed the case for sodium clusters [59]). However, it has been shown that the hard sphere approximation does not introduce significant errors in the nucleation rates, as far as detailed balance is used to calculate evaporation rates [59], which is the case here as shown in the next paragraph. Recent experiments have shown that the hard sphere model is a good approximation for the attachment cross sections of water clusters, except for very small sizes (below about ten molecules) for which inelastic collisions significantly reduce the sticking efficiency [60]. This is of no consequence here since such small clusters are out of the validity range of the present model.

The condensation term R_c must be integrated over the stochastic fluctuation x. The only nonvanishing terms are

$$R_c\langle n+1,\varepsilon' | n,\varepsilon\rangle = \int_{-\infty}^{+\infty} dx \beta(T,\varepsilon) A(n) \delta(\varepsilon' - [\varepsilon + q + x]), \tag{10}$$

which corresponds to the attachment of a molecule onto a cluster of initial size n and fluctuation energy ε, and a similar term for the attachment of a molecule onto a cluster of initial size $n-1$.

The evaporation rate R_v is more difficult to estimate. It is evaluated invoking the principle of detailed balance: at equilibrium, the sticking rate exactly compensates the evaporation rate,

$$\Gamma(n,\varepsilon,x) c_0(n,\varepsilon) = \beta(T,x) A(n-1) c_0(n-1,\varepsilon - q - x), \tag{11}$$

where $\Gamma(n,\varepsilon,x)$ is the evaporation rate of a cluster of size n and fluctuation energy ε, emitting a fragment of fluctuation energy x. $c_0(n,\varepsilon)$ is the equilibrium population of a cluster of size n and fluctuation energy ε. The total evaporation rate $R_v\langle n-1,\varepsilon' | n,\varepsilon\rangle$ for a cluster of size n and internal energy ε toward a cluster of size $n-1$ and internal energy ε' is

$$\begin{aligned} R_v\langle n-1,\varepsilon' | n,\varepsilon\rangle &= \int_{-\infty}^{+\infty} dx \Gamma(n,\varepsilon,x) \delta(\varepsilon' - [\varepsilon - q - x]) \\ &= \int_{-\infty}^{+\infty} dx \left\{ \beta(T,\varepsilon) A(n-1) \right. \\ &\quad \left. \times \frac{c_0(n-1,\varepsilon - q - x)}{c_0(n,\varepsilon)} \delta(\varepsilon' - [\varepsilon - q - x]) \right\}. \end{aligned} \tag{12}$$

It can be noted that the cluster decay rate $\Gamma(n,\varepsilon,x)$ depends here on the temperature of the vapor. Barrett considered this dependence as erroneous [34]. However, it is worth noting that this dependence is inherent to the detailed balance assumption, which is widely considered as a key to nucleation theory. The detailed balance principle consists in assuming that, in a reaction, the relative population of the initial and the final states is equal to the ratio of the density of states in the phase space. This is the basis of the Weisskopf model, widely used to describe the evaporation of clusters [61,62]. In the evaporation process, the initial state is the cluster of size n and the final state a cluster of size $n-1$ *plus* the evaporated molecule; thus, the total density of states of the final state includes the density of states of the evaporated molecule. The density of states of the evaporated molecule depends on its translational energy. At equilibrium, the mean value of this translational energy is the mean energy of the molecules of the vapor, determined by its temperature. Therefore, since $c_0(n,\varepsilon)$ represents an equilibrium population, there may be a relation between the clusters decay rate and the temperature of the vapor.

It is actually the way described above for eliminating the evaporation rate from the equations that introduces the so-called supersaturation parameter. Such an elimination is valid as far as the sticking rate is strictly proportional to the supersaturation, which holds except at very high pressure [3,4]. So far only the properties of the statistical energy fluctuation x of the impinging molecules have been involved and no particular assumption has been made concerning the internal energy of the droplets or the equilibrium population $c_0(n,\varepsilon)$.

Expressions (10) and (12) can now be inserted into Eq. (8). By replacing the difference terms $f(n) - f(n-1)$ with differential terms $df/\partial n$ and by integrating over ε' before integrating over x, the following differential (diffusion) equation is obtained:

$$\frac{\partial c(n,\varepsilon)}{\partial t} = \vec{\nabla} \cdot \{ D c_0(n,\varepsilon) \cdot \vec{\nabla} [c(n,\varepsilon)/c_0(n,\varepsilon)] \}, \tag{13}$$

where

$$D = \beta_n \begin{pmatrix} 1 & q \\ q & b^2 + q^2 \end{pmatrix}$$

is a two-dimensional diffusion tensor. β_n is a shorthand notation for $\beta(T,\varepsilon)A(n)$ that is independent on both ε and T within the hard sphere approximation. q is given by relation (9) (the size-dependent term $\sigma \partial A(n)/\partial n$ can be neglected in

a first approach [1]). The term b, which accounts for the energy removed by inelastic collisions, is given by the following relation [1]:

$$b^2 = \left(c_V + \tfrac{1}{2}k_B\right)k_B T^2 + \kappa\left(c_{V,C} + \tfrac{1}{2}k_B\right)k_B T^2, \tag{14}$$

where c_V and $c_{V,C}$ are the molecular heat capacities of the condensable and the carrier gas, respectively. The effect of a carrier gas, which has been neglected so far, has been straightforwardly introduced in the term b, which accounts in the same way for the energy removed by inelastic collisions with both the condensable vapor (first term) and the carrier gas (second term) [1]. The factor κ in the second term is the ratio of the impingement frequencies of the carrier gas to the one of the condensable gas: if one assumes that the collision cross section with a cluster does not vary significantly from the condensable to the carrier gas molecules, κ is approximately the ratio of the carrier gas pressure to the condensable gas one.

The diffusion tensor D is not diagonal and the dynamics along the two coordinates n and ε are correlated, which prevents from any interpretation without a full calculation of the dynamics. The solution is to use a new system of coordinates $\{u,v\}$ instead of $\{n,\varepsilon\}$, in which the diffusion tensor D is diagonal. Such coordinates can be found within the approximation of a constant q value. The nontrivial coordinate transformation, which does not appear in Feder's original paper, is developed in the Appendix. It is important to check that the coordinate transformation remains valid for any distribution c_0 since the equilibrium population c_0 will be modified in the following with respect to the one used in Feder's original paper. The v coordinates depends only on the internal energy, whereas u depends on both energy and size. However, u becomes rapidly very close to n as the size increases, so we will often refer in the following to the u coordinate as a "size" coordinate.

In the $\{u,v\}$ space, the nucleation process is strictly equivalent to an isotropic thermal diffusion whose properties are better documented. In particular, the flux follows the gradient of the free-energy surface, which is not generally the case when the stochastic motions along the two coordinates are correlated.

The nucleation flux J in the $\{u,v\}$ space is given by Fick's law,

$$\vec{J} = -D' c_0'(u,v) \cdot \nabla'[c'(u,v)/c_0'(u,v)]. \tag{15}$$

The vectorial flux $\vec{J}$ has now two uncoupled components J_u and J_v along the two coordinates. As far as the melting transition is not considered, the nucleation path is found to be a valley whose minimum makes a very small angle with respect to the $\varepsilon=0$ axis: the nucleation paths are almost parallel to the u axis. They must nevertheless be integrated over all internal energies, and the total nucleation rate J is

$$J = \int_{-\infty}^{+\infty} J_u dv, \tag{16}$$

which is to a good approximation equal to

$$J \approx \frac{b^2}{b^2 + q^2} J_{ISO}, \tag{17}$$

where J_{ISO} is the isothermal nucleation rate given by relation (5).

So far we could set aside the question of giving an expression for the equilibrium population c_0, which implicitly shows that all the previous developments can be done independently of any particular choice for this quantity. In Feder's model, c_0 is deduced, using standard physical arguments [3,4], from the relation between the equilibrium population and the free energy of formation of a droplet ΔG^0. ΔG^0 is related to the equilibrium population $c_0(n,\varepsilon)$ by

$$\Delta G^0(n,\varepsilon) = -k_B T \ln[c_0(n,\varepsilon)/c(1)]. \tag{18}$$

As far as melting is not considered, $c_0(n,\varepsilon)$ is written in a standard Gaussian fluctuation approximation,

$$c_0(n,\varepsilon) = c_0(n) H(n,\varepsilon,T),$$

$$H(n,\varepsilon,T) = (2\pi n c_m k_B T^2)^{-1/2} \exp(-\varepsilon^2/2nc_m k_B T^2), \tag{19}$$

where c_m is the molecular heat capacity of the cluster.

Nucleation is described as a diffusion motion in the free-energy landscape $\Delta G^0(u,v)$. $\Delta G^0(u,v)$, as calculated by Feder *et al.*, exhibits a valley whose bottom is followed in the nucleation process. The bottom of the valley first increases with the u coordinate up to a saddle point at u^* (equivalent to the critical size in CNT) and then decreases for $u > u^*$. The minimum of the free energy along the v coordinate is found at negative v values for $u < u^*$ and positive v values for $u > u^*$: droplets are colder than the vapor before the critical size and warmer above.

It is informative to rewrite Eq. (13) using relation (18): It shows more clearly that the nucleation process can be seen as a thermal diffusion motion in a field of force $-\vec{\nabla}\Delta G^0(u,v)$: the equation of evolution is a thermal diffusion-drift *Fokker-Planck* equation

$$\frac{\partial c}{\partial t} = \vec{\nabla} \cdot D\left[\frac{c}{k_B T}\vec{\nabla}(\Delta G^0)\right] + \vec{\nabla} \cdot (D\vec{\nabla}c), \tag{20}$$

where k_B is the Boltzmann constant and T is the temperature of the vapor. The first term is the drift component and the second is the diffusion component.

C. Solid-liquid transition in growing droplets

Since the free energy ΔG^0 is determined from the equilibrium population [relation (18)], the melting of the droplets can be introduced by replacing the distribution $H(n,\varepsilon,T)$ given by relation (19) with the distribution $F(n,\varepsilon,T)$ given by relation (4). $c_0(n)$, which depends only on growth and decay rates [3,4], is unchanged. This approximation is justified insofar as the growth rate is hardly modified from liquid to solid [59] and the change in the decay rate can be accounted for by the energy shift $\varepsilon_L = \varepsilon - nL$ in relation (4) [46]. This energy shift is equivalent to assuming that the latent heat of sublimation is equal to the latent heat of evaporation plus the latent heat of melting. Using the relation between

u,v and n,ε (given in the Appendix) and replacing $H(n,\varepsilon,T)$ with $F(n,\varepsilon,T)$, $\Delta G^0(u,v)$ is obtained from relation (18) as follows:

$$\Delta G^0(u,v) = -k_B T \ln\{c_0[n(u,v)]/c(1)\} - k_B T \mathrm{Ln}F[n(u,v),\varepsilon(u,v),T]. \quad (21)$$

The first term of the right member, which does not depend on ε, is just the standard isothermal free energy of formation. We chose the most widely used expression in the capillarity approximation [3,4], and some additional terms introduced by Feder and co-workers have been dropped; these (small and controversial) terms introduce negligible changes in $\Delta G^0(u,v)$. Finally, the expression of $\Delta G^0(u,v)$ used here is

$$\Delta G^0(u,v) = -n(u,v)k_B T \ln S + \sigma A[n(u,v)] - k_B T \mathrm{Ln}F[n(u,v),\varepsilon(u,v),T]. \quad (22)$$

The present study cannot deal with very small sizes, for which the capillarity approximation for both melting and nucleation is known to fail. Experiments on clusters have suggested that droplets can be described in the frame of the capillarity approximation down to sizes on the order of 10^2 atoms or molecules [47]. On the other hand, nucleation theories cannot describe the growth of very large droplets, for which coalescence and vapor depletion can no longer be neglected [1,3,4] ($n\to\infty$ will refer to this limit in the following). This limit depends on the nature of the condensable vapor and the saturation conditions. For water under atmospheric conditions, its order of magnitude has been estimated to 10^{11} [1]. The validity range of our model might even be reduced to smaller sizes, as shown below.

We will emphasize now the specific nature of the solid-liquid phase transition of *growing* droplets. For small growing droplets, this transition does not proceed as in the bulk. We will point out here the main peculiarities of the phase transitions in growing droplets, in comparison with the canonical first-order phase transition in the thermodynamic limit of infinite size and infinite time of equilibration. First, for small systems, as shown in Sec. III A, the melting transition gradually occurs over a temperature range in which solid and liquid clusters coexist, whereas in the bulk the transition is sharp (the temperature range of coexistence tends to zero). Second, growing particles cannot be described in the frame of the canonical ensemble, where the temperature if fixed and energy is instantaneously available from the thermostat (a review of the differences between canonical and microcanonical descriptions of first-order phase transitions can be found in [53]). During nucleation, energy is brought to the droplets only by collisions with the molecules of the vapor. The internal equilibration time of a small droplet (here, the relevant time scale is given by the mean thermal vibration frequency $k_B T/h$, where h is Planck's constant [38,63]) is generally much smaller than the mean time between collisions [63]. The droplets are better described in the frame of the microcanonical ensemble, with stochastic variations of their internal energy due to collisions, on a slow time scale compared with droplets internal relaxation time. In the microcanonical ensemble, small systems can reach states with any energy between the solid and the liquid, which is not allowed for large system in the canonical ensemble [53]. In our model, the free-energy barrier between solid and liquid is implicitly given by the bimodal shape of internal energy distribution shown in Fig. 1 [56].

Finally, as far as internal relaxation is fast with respect to the collision frequency, the solid-liquid kinetics is correctly described by our model as a diffusion process on the free-energy surface ΔG^0. However, there is an intrinsic limitation of any growing model based on the free energy where the effects of energy and entropy are undistinguishable: as a matter of fact, the kinetics of solid to liquid and liquid to solid transitions are considered symmetrically in the model, which is actually not correct [64]: the solid must overcome an energy barrier to melt, whereas the liquid must overcome an entropic barrier to freeze, with a slower kinetics. This is responsible for a difference between melting and freezing temperatures, even in clusters [63,65,66]. This cannot be accounted for in our model where melting and freezing temperatures are equal. For small droplets, as far as the internal relaxation is much faster than the collision rate, it is of no consequence. For very large droplets, however, the collision cross section—and therefore the collision frequency—increases, whereas the internal relaxation time of the whole droplet increases and can no longer be considered as negligible. An order of magnitude of the size from which the internal relaxation time can no longer be neglected is given by the size at which the collisions frequency and the mean thermal vibrational period $k_B T/h$ are equal. For water at 253 K at the saturation vapor pressure ($\sim 10^2$ Pa), this size is about 5×10^9 (this size increases with decreasing the temperature). From this size, the freezing kinetics being slower than the melting one should be explicitly considered in a rigorous treatment, and the present model overestimates the freezing rate. Accounting rigorously for the freezing kinetics of large droplets is out of reach of our model; first because of the fundamental reasons mentioned above and second because the freezing kinetics is highly system dependent and, even for a given element, it is expected to depend on the structure of the solid phase. For water, for instance, it would certainly depend on whether cubic, hexagonal, or amorphous solid water is formed.

To sum up, our model is likely to give a satisfactory description of the solid-liquid transitions of growing droplets for small sizes and is more questionable for very large droplets. However, first the threshold between "small" and "large" sizes is rather large; second, although the transition probability between liquid and solid droplets is expected to be modified, qualitative features such as the existence of two growing channels are not likely to disappear in a more rigorous treatment. A major conclusion of this work, the fact that droplets often grow preferentially in the liquid state even at temperatures lower than the melting temperature, would even be reinforced since our model overestimates the liquid to solid transition rate of very large droplets. Another peculiar feature, which will be demonstrated in Sec. IV, is the existence of potential wells responsible for finite-size metastable droplets. Although the exact shape of these potential wells may be modified, they are unlikely to disappear in a more accurate treatment. In order to simplify the discussion, liquid and solid droplets will be distinguished in the following on the basis on their internal energy.

IV. INTERPLAY BETWEEN NUCLEATION AND MELTING IN WATER VAPOR

Nucleation of water droplets is analyzed as a case study. The most remarkable effect is the enhancement of the probability to find droplets in the liquid state. This is qualitatively easily understood: droplets are heated in the nucleation process due to unreleased heat of association. Therefore, high internal energy states are more populated than at equilibrium and, even at vapor temperatures below their melting temperature, droplets often grow preferentially in the liquid state.

$\Delta G^0(u,v)$ has been calculated for water droplets under various temperature and supersaturation conditions. Although $\Delta G^0(u,v)$ represents an equilibrium free energy, one must bear in mind that the population of the growing particles is *not* merely proportional to the equilibrium Boltzmann factor $\exp[-\Delta G^0(u,v)/k_BT]$ but is the nonequilibrium constant flux solution of Eq. (20). When the gradient of $\Delta G^0(u,v)$ is negative along the growth path, the motion is dominated by the drift term, whereas the diffusion term dominates in the directions of increasing $\Delta G^0(u,v)$. On average, the nucleation flux flows along the direction of the gradient of $\Delta G^0(u,v)$. The actual trajectories can move away from this mean path due to stochastic thermal motions, but essentially in a limited energy range on the order of k_BT above the bottom of the potential [1].

Figure 2 displays a typical free-energy landscape. The introduction of melting in the nucleation model gives rise to two distinct nucleation channels, corresponding to solid and liquid states, respectively (within the restrictions of Sec. III C). A saddle point must be overcome along the nucleation path (along the u coordinate) and defines a critical size in the usual meaning. The critical size can be crossed either in the liquid state (Fig. 2) or in the solid state (Fig. 3). Along the v coordinate, a free-energy barrier separates solid and liquid channels. In the present work, this barrier is generally far higher than k_BT. Kramers approximation [53] can be used to estimate the probability to overcome this barrier. At least in the drift regime beyond the critical size, the transition probability from one channel to the other is negligible as far as the height of the barrier is much higher than k_BT. The classical Kramers parabolic approximation that gives the rate coefficient for barrier crossing due to thermal activation is of the form $K\exp(-E_b/k_BT)$, where E_b is the height of the barrier [67]. The kinetic prefactor K, which is overestimated by the vibrational frequency at the bottom of the free-energy well, is roughly the frequency at which the system tries repeatedly to overcome the barrier (note that, according to the hypothesis made in Sec. III C, one considers here that the limiting kinetic factor is the collision frequency, not the internal vibrational frequency). The complex free-energy surfaces encountered in our case are not always well approximated (near their extrema) by harmonic wells or barriers, but it has been shown that, in thermal diffusion, the shape of the barrier does not play a major role: the order of magnitude of K is not strongly modified even in the case of square potentials [68]. It is convenient to define a time scale where the attachment coefficient β_n is unity. Within this convention, the mean time to grow by one unit along the u coordinate is

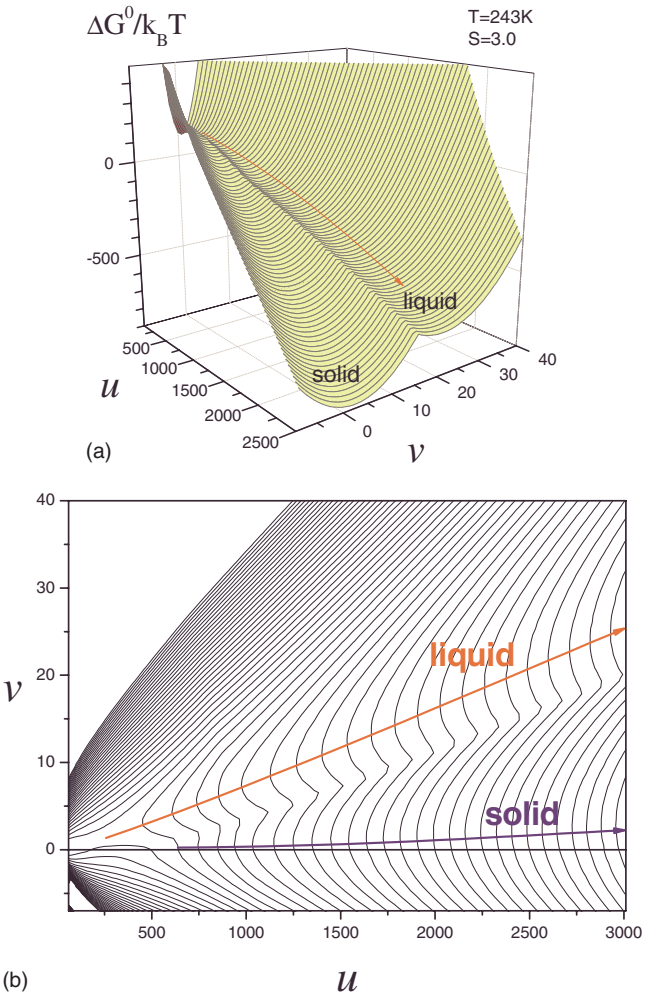

FIG. 2. (Color online) (a) Nucleation path on the free-energy surface $\Delta G^0(u,v)$ at $T=243$ K, $S=3$, and $\kappa=0$. The critical size is crossed here in the liquid state. (b) Contour plot of the same energy surface. The arrows follow the bottom of liquid and solid growing channels.

about $b^2/(b^2+q^2)$ [1]. In the limit of isothermal nucleation (i.e., when the partial pressure of buffer gas is high enough), this factor is asymptotically unity, whereas it is on the order of 10^{-2} for water with no buffer gas. The probability to overcome a barrier (along the v coordinate) is about $\exp(-E_b/k_BT)$ since here the frequency at which the system tries to overcome the barrier is simply given by the collision rate. Finally, the integrated probability P_b to overcome a barrier of constant height E_b during the growth over a size range N is at most

$$P_b \approx N\frac{b^2+q^2}{b^2}\exp(-E_b/k_BT). \tag{23}$$

Because of the exponential term, this probability can remain tiny even over a huge N range. The prefactor in relation (23) being a crude estimate is not important for our purpose since the order of magnitude of P_b is essentially determined by the exponential. Relation (23) will be useful later to show that in particular cases droplets can be trapped in the liquid

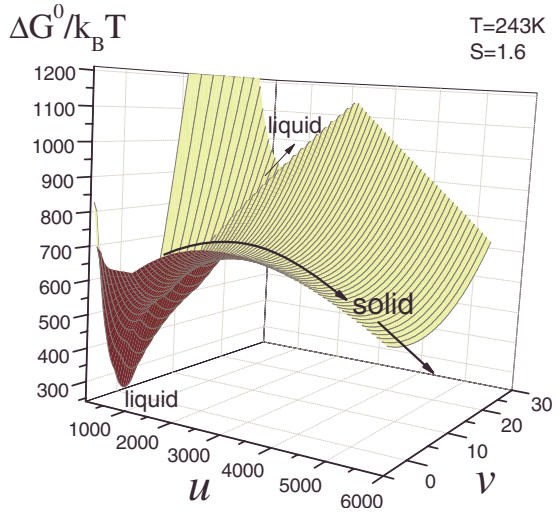

FIG. 3. (Color online) Nucleation path on the free-energy surface $\Delta G^0(u,v)$ at $T=243$ K, $S=1.6$, and $\kappa=0$. Along the minimum-energy path, the saddle point is crossed in the solid phase.

channel up to very large sizes. In short, beyond the critical size the phase of all droplets is well defined in most cases since the transition probability from one channel to the other is generally very small.

In subcritical regions (for $u<u^*$), where clusters move by diffusion in any direction, there is no such a clear time scale separation between the motions along u and v directions. The minimum-energy path defines the path followed by the droplets that will eventually overcome the critical size, but a population of liquid droplets can exist below u^* even when the critical size is crossed in the solid state, and conversely. Moreover, finite-size broadening of the valleys at small sizes can give rise to a statistical mixing of solid and liquid particles. Finally, although the path followed by droplets that will pass the critical size can generally be known unambiguously, the thermodynamic phase of subcritical droplets is often not as well defined as it is above the critical size. Thus, in the following, the phase of subcritical clusters must be understood as the phase of clusters that will actually reach the critical size, and one must bear in mind that a population of clusters that will never grow may also exist in a different phase. Note that if the whole size range of droplets is considered (from dimers up to the limit of validity of the model as defined previously), subcritical clusters represent a tiny fraction of the whole population.

Except the special cases studied in Sec. IV B, liquid and solid channels are well separated near the critical size. Two critical sizes can often be defined, each defined by a saddle point, one in the liquid channel and the other in the solid one. However, the saddle point that has been crossed by supercritical droplets is defined unambiguously in most cases. Let us assume, for instance, that the saddle point in the liquid phase lies ΔE above the saddle point in the solid phase. In this case, since subcritical clusters grow only by diffusion, the probability for overcoming the solid saddle point is greater than the probability for overcoming the liquid saddle point by about $\exp(\Delta E)$, which is usually a huge quantity.

A. Nucleation energy landscapes: Melting far from the critical size

Let us now analyze some particular features in the nucleation process due to the phase transition. The solid channel, as far as it exists, looks like the single valley obtained by Feder and co-workers without melting: its bottom is below the $v=0$ axis before the critical size and above this axis beyond that size, which means that the droplets are colder and warmer than the vapor, respectively. The solid channel does not necessarily exist from $n=1$ (see Fig. 3). At very low temperature and low supersaturation, the liquid channel can disappear above a finite size. The bottom of the liquid channel approximately follows a curve defined by $\varepsilon_L \approx nL(n)$. The cooling and heating effects before and after the critical size, reported above for the solid channel, also exist in the liquid state but is negligible compared to $nL(n)$. L varies smoothly with u; thus, the bottom of the liquid channel is locally well approximated by a straight line of slope $b/(b^2+q^2)\times uL(u)$ [see Fig. 2(b)]. At very small sizes (depending on S, but typically about a few tens), the two channels can no longer be distinguished, because of finite-size broadening of the internal energy distribution and of the transition temperature range accounted for by θ [see relations (3) and (4)].

Down to temperatures on the order of the equilibrium melting temperature of very small droplets (~200 K), except for very low S values, particles start growing preferentially in the liquid state even in cases where the critical size is crossed in the solid state, as in Fig. 3. At some size, before or after the saddle point, the solid valley becomes energetically more favorable [see Fig. 2(a)]. Nevertheless, the droplets do not necessarily reach the solid state above this size because of the free-energy barrier between liquid and solid channels. At even larger sizes, either the liquid channel can disappear or both liquid and solid channels can coexist up to infinite u values. The liquid to solid transition size n_T can be estimated by the size at which the free-energy barrier between liquid and solid is equal to k_BT. In this case, relation (23) ensures that the probability to overcome the barrier after a few collisions becomes significant. The variations of n_T as a function of S at several vapor temperatures are shown in Fig. 4. n_T strongly increases with S: the transition from liquid to solid does not merely occur at the size n for which $T_{melt}(n)=T_{vapor}$. This result is consistent with Monte Carlo simulation of water nucleation, in which critical nuclei exhibit liquidlike structure between 200 and 300 K [69]. For a particular set of (S,T_{vapor}) couples, the melting temperature at the critical size is equal to the vapor temperature: in this case the transition from solid to liquid simply occurs at the size for which the melting temperature is equal to the temperature of the vapor. Since the angle of propagation in the (u,v) plane is very small even in the liquid channel, Feder's argument still applies and the critical size is not significantly modified with respect to the standard isothermal value (see for instance [4]),

$$n^* = \frac{v_m^2\sigma^3}{(k_BT\ln S)^3}, \tag{24}$$

where v_m is the molecular volume.

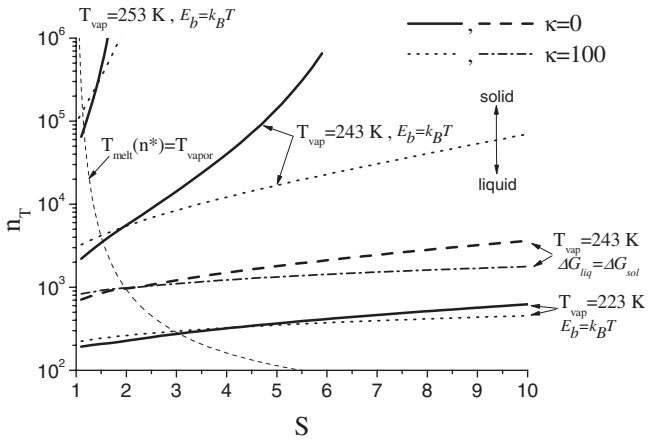

FIG. 4. Liquid to solid transition size n_T as a function of supersaturation for different vapor temperatures, without (solid lines) and with (dotted lines) carrier gas, respectively. Droplets are liquid below the lines and solid above. For the curves labeled $E_b=k_BT$, the transition size is defined as the size for which the barrier between the solid and the liquid channels becomes lower than k_BT. At 243 K are also represented the limits defined by $\Delta G^0_{solid}=\Delta G^0_{liquid}$ without (thick dashed line) and with (dashed-dotted line) carrier gas.

The set of (S,T_{vapor}) critical values (see Fig. 4) are then easily obtained from relations (1) and (24) by assuming

$$T_{melt}(n^*) = T_{vapor}. \tag{25}$$

(S,T_{vapor}) critical values are independent of the amount of carrier gas since the droplets at the critical size are by definition at equilibrium with the vapor.

A general effect of nucleation is that the droplets are increasingly likely to be liquid as S increases. It can be qualitatively understood: the mean time between two collisions decreases as the pressure increases; and clusters with a higher internal energy, and then shorter decay times, can grow. It is quantitatively more complex since the internal energy E_i behaves differently for $u>u^*$ and for $u<u^*$. Let τ_E be the mean evaporation time and τ_C the mean time between two collisions. At equilibrium (at u^*), $\tau_E=\tau_C$. For $u>u^*$, $\tau_C<\tau_E$ and droplets can undergo several collisions without evaporating: the mean value of E_i is higher than at equilibrium. τ_C is a decreasing function of S. The evaporation time τ_E does not depend on S and is a decreasing function of E_i. Thus, the maximum allowed value of E_i, determined by the condition $\tau_{E_i}=\tau_C$, is an increasing function of S. For $u<u^*$, high S values also favor the liquid state, but growth only occurs through favorable energy fluctuations (since $\tau_C>\tau_E$ on average) and the relation between S and E_i is more complex. Qualitatively, however, it is clear that the colder a droplet, the larger its probability to reach the critical size: the mean internal energy of growing droplets below the critical size is lower than its average equilibrium value, as already pointed out by Feder and co-workers [1].

The transition from liquid to solid state does not necessarily occur at a finite size. From a critical temperature (below the bulk melting point) that depends on S, the height of the potential barrier between the liquid and the solid valleys always remains much larger than k_BT up to very large sizes.

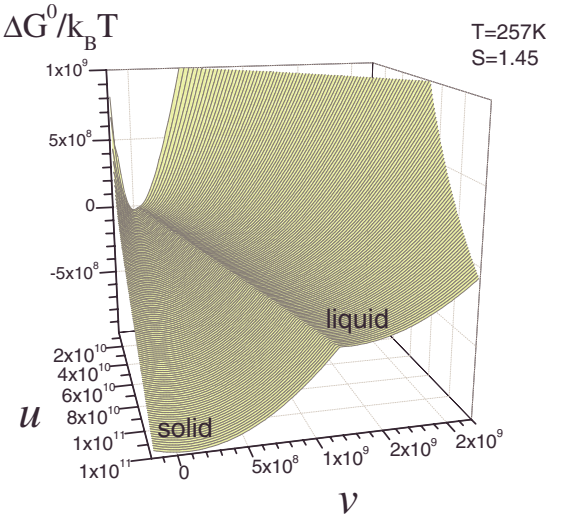

FIG. 5. (Color online) Free-energy surface $\Delta G^0(u,v)$ at $T=257$ K and $S=1.45$. Droplets can reach infinite size in a metastable liquid state.

An example of such a behavior is shown in Fig. 5 at a temperature of 257 K and a supersaturation of 1.45. The critical size is crossed here in the liquid state (u^* is about 5000). At very large sizes the solid valley becomes energetically favored: at equilibrium, large droplets would be solid. However, there is a free-energy barrier between liquid and solid paths from the critical size up to the largest size $n=10^{11}$. The height of the barrier at $n=5000$ is about $250k_BT$ and is much higher at $n=10^{11}$. The transition probability can be overestimated by considering a barrier of constant height equal to its value at the critical size. According to relation (23), the probability to reach the final size in the solid state is overestimated by $10^{11}\exp(-250)\approx 3\times 10^{-98}$ [the factor $(b^2+q^2)/b^2$, which is clearly insignificant here, has been dropped]. In this typical example an overwhelming majority of droplets reach the final size in the liquid state. The approximate limit from which the phase of the final state (at $n\to\infty$) is liquid, estimated from the condition $E_b(n\to\infty)<k_BT$, is plotted in Fig. 6. Of course, the droplets must also have crossed the saddle point in the liquid state. This condition, given by relation (25), is fulfilled as far as the free energy is lower at the liquid saddle point than at the solid saddle point. It does not depend on the amount of carrier gas.

The properties (the curvature, for instance) of ΔG^0 in the vicinity of u^* are nearly independent of the thermodynamic phase. Insofar as the solid and the liquid valleys are well separated near u^*, the first (second) term in relation (4) can be dropped; in other words, the droplets are clearly liquid (solid) at the critical size. Even if ε is larger in the liquid state, v remains small compared to u; thus, the angle of the propagation path with respect to the u axis remains small. The curvature of the potential close to u^* is also only very slightly modified, thus the equivalence of the Zeldovich prefactor of CNT. Finally, if the phase transition takes place far from the critical size, the effect of melting on the nucleation rate is not expected to be important; the arguments of Feder *et al.* still apply, and J is well approximated by relation (10). For the same reasons the critical size is still well approximated by relation (24).

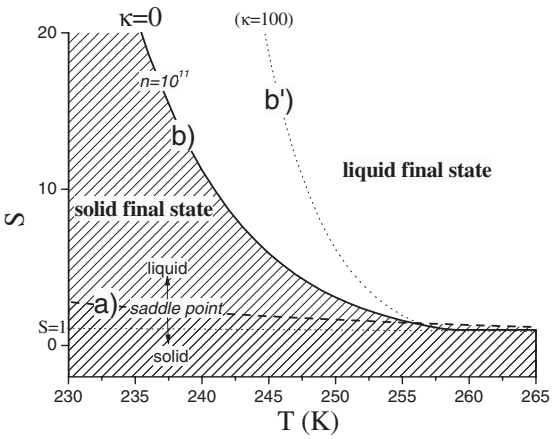

FIG. 6. Approximate critical S value from which the droplets reach "infinite" size ($n=10^{11}$, see text) in the liquid state, plotted as a function of the vapor temperature. Two conditions are required: (a) the droplets pass the critical size in the liquid state (dashed line a). This limit is independent of κ. (b) The height of the barrier between liquid and solid channels at $n=10^{11}$ is greater than k_BT. This limit is shown without buffer gas ($\kappa=0$, solid line b) and for a partial pressure of condensable vapor on the order of 1% ($\kappa=100$, dotted line b').

B. Nucleation energy landscapes: Melting near the critical size

Cases where the solid-liquid transition occurs in the vicinity of the saddle point are more complex. They can be rationalized by plotting the minimum-energy path as illustrated in Fig. 7. A threshold value S_T separates two regimes. For $S<S_T$, the critical size is determined by the maximum of ΔG^0 in the solid state (as in Fig. 3), whereas at $S>S_T$ the free-energy maximum in the liquid state determines the critical size (as in Fig. 2). The transition between these two regimes occurs when $T_{melt}(n^*)=T_{vapor}$. In a small S range (typically $\pm 1\%$ S_T) around S_T, the saddle point is imposed by the height of the barrier between liquid and solid, as illustrated in Fig. 8. In all cases, in this transition region, the activation barrier is increased with respect to the standard one. The difference is significant only in a small range around S_T (typically $\pm 5\%$ S_T), but can be very important. For instance, at $T_{vapor}=243$ K, $\kappa=0$ ($S_T\approx 2.05$), it reaches more than $35k_BT$ at S_T. From relations (5) and (17), the corresponding difference in the nucleation rate is roughly 15 orders of magnitude. This estimate does not take into account the change in the Zeldovich prefactor, which cannot be evaluated on such complex surfaces. Even if the prefactor is not well known, its influence on J is certainly much smaller than that of the argument of the exponential and the nucleation rate is certainly damped near S_T. Another interesting feature is the existence of solid and liquid wells for specific S values slightly lower and slightly larger, respectively, than S_T. Both wells are much deeper than k_BT and really give rise to metastable liquid and solid finite-size droplets. Such metastable wells are shown in Fig. 9.

Let us finally briefly analyze the effect of the carrier gas, characterized by the value of κ [see relation (14)]. $\kappa=0$ corresponds to the absence of carrier gas. Without melting, the effect of κ has already been analyzed by Feder and co-

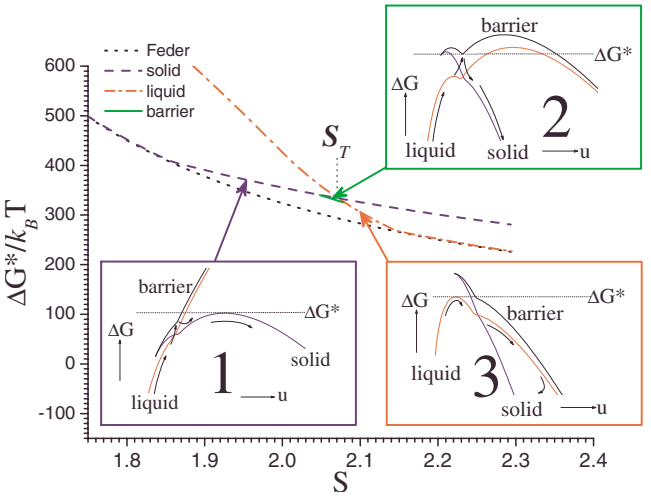

FIG. 7. (Color online) Free-energy maximum ΔG^* along the minimum-energy path as a function of supersaturation near the critical value, calculated for water at 243 K and for $\kappa=0$ (no buffer gas). Three different cases are observed, depending on the value of S compared with the threshold value S_T, for which liquid and solid free energies at the critical size are equal. (1) Dashed (blue online) line: the maximum is crossed in the solid state (see Fig. 3); (2) solid (green online) line: the maximum is determined by the barrier between solid and liquid states (see Fig. 8); (3) dashed-dotted (red online) line: the maximum is crossed in the liquid state (see Fig. 2). The dotted black line labeled "Feder" is calculated without melting transition using relation (17).

workers. Figure 10 displays the evolution of the transition size n_T as a function of the amount of carrier gas. The variation of the transition size with S is damped but remains significant up to κ values on the order of 10^3. In experiments or practical cases κ is often much lower than 10^3: in cloud chamber experiments on water [28] or in the atmosphere κ is on the order of 10^2 [1]. Of course, when the partial pressure of the carrier gas is very high ($\kappa\to\infty$), thermal equilibrium is achieved: the curves in Fig. 10 converge to straight lines parallel to the abscissa. The variations of n_T as a function of

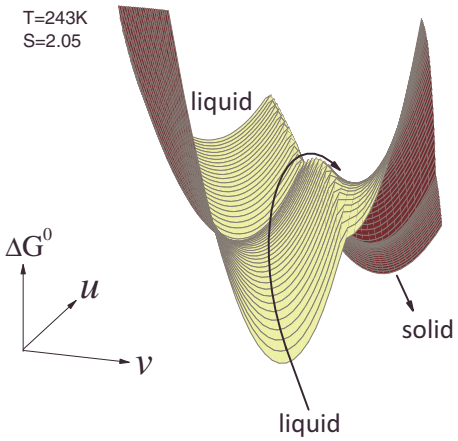

FIG. 8. (Color online) Nucleation path at $T=243$ K, $S=2.05$, and $\kappa=0$. In this critical case [case (2) in Fig. 7], the barrier between solid and liquid channels determines the minimum-energy path.

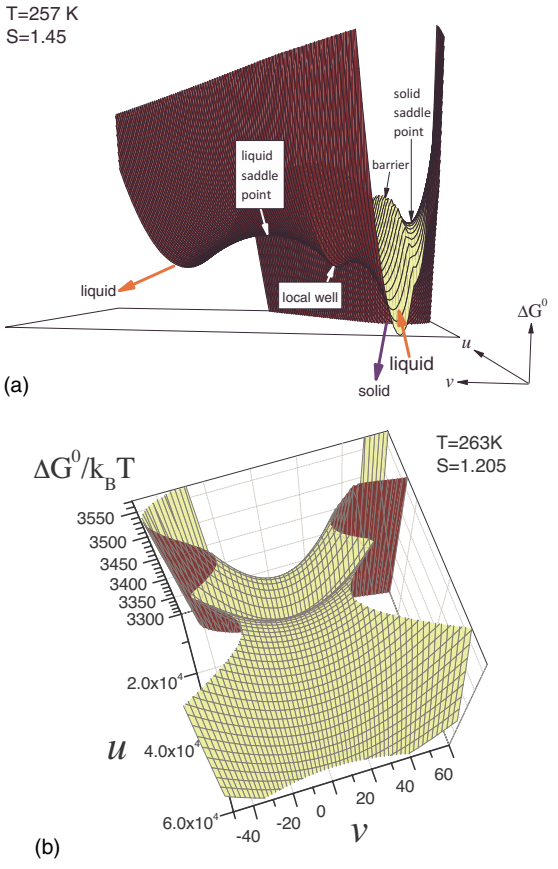

FIG. 9. (Color online) Examples of metastable wells on the free-energy surface $\Delta G^0(u,v)$ (a) in the liquid state and (b) in the solid state.

S for $\kappa=100$ plotted in Fig. 4 show that the phase properties described previously are not qualitatively modified. The evolution of the transition size with κ is more easily understood when setting aside the effect of the barrier, i.e., assuming the transition condition $\Delta G^0_{solid}=\Delta G^0_{liquid}$. The transition sizes n_T follow the same trends as for $\kappa=0$ but the transition is shifted to lower sizes. As shown in Fig. 4 at 243 K, the curves just rotate with only a slight deformation around a fixed point

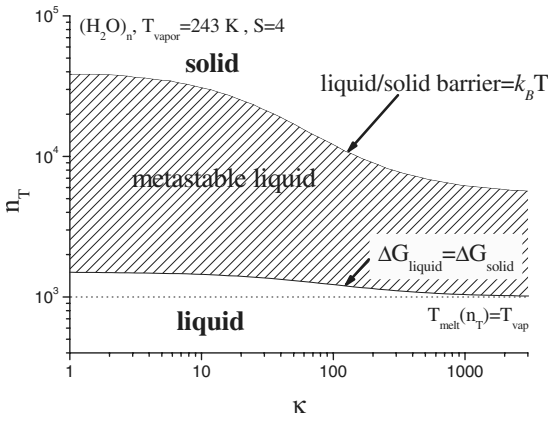

FIG. 10. Liquid to solid transition size as a function of the amount of carrier gas. κ characterizes the number of collisions with the carrier gas between two collisions with the condensable gas.

defined by relation (25). Thermalization to the vapor temperature requires high κ values, at least on the order of 10^3.

V. CONCLUSION

A theoretical model is developed to describe the interaction between nucleation, melting, and freezing of droplets in supersaturated vapors. The model combines a size-dependent description of the melting transition based on recent findings in cluster physics [7] and the two-dimensional nonisothermal nucleation model developed by Feder *et al.* [1]. The solid or liquid character of the droplets is inferred from their internal energy distribution. This approximation is valid as far as the melting and freezing kinetics of the droplets is fast in comparison with the collision rate. The interplay between growth and melting is exemplified in the case of water. The two-dimensional free-energy landscape that determines the growing properties generally exhibits two nucleation paths corresponding to solid and liquid droplets, respectively. The position, shape, possible crossing, and energy barrier between liquid and solid paths depend on both the temperature and the pressure of the vapor in a nontrivial way, but a few general features arise: the energy released in attachment heats the droplets and favors their growth in the liquid state even at vapor temperatures far below their melting point. It is shown that the higher the supersaturation, the higher the probability to grow in the liquid state. Our theoretical work support the experimental results by Anderson and co-workers on homogeneous nucleation of water vapor at low temperature (down to −50 °C), which strongly suggest that ice nucleation occurs as a result of homogeneous nucleation of liquid droplets which *subsequently* mature to macroscopic ice particles [37]. The solid-liquid phase transition is shown to give rise to metastable finite-size droplets, trapped in free-energy wells either in the liquid or in the solid state.

The present study—although speculative to some extent—may open the way for challenging experiments, for instance, the observation of a pressure-induced transition from liquid to solid at constant vapor temperature. It might also be of interest in atmospheric physics. Under certain pressure and temperature conditions encountered in the atmosphere, droplets might reach naturally very large sizes in the liquid state at temperatures far below 0 °C.

ACKNOWLEDGMENTS

The author is grateful to Pierre Labastie for many stimulating discussions and to Christine Lauzeral for mathematical assessments.

APPENDIX: DIAGONALIZATION OF THE DIFFUSION TENSOR

It is convenient to rewrite Eq. (13) using the variables p, $\mathfrak{D}$, B, and V, defined as follows:

$$p = c_0 \beta A(n),$$

$$D = \beta A(n) \begin{pmatrix} 1 & q \\ q & b^2 + q^2 \end{pmatrix} = \beta A(n) \mathfrak{D},$$

$$B = p\mathfrak{D},$$

$$V = \vec{\nabla}(c/c_0) = \begin{pmatrix} \frac{\partial c/c_0}{\partial n} \\ \frac{\partial c/c_0}{\partial \varepsilon} \end{pmatrix}.$$

These variables are defined here in the $\{n,\varepsilon\}$ space. The variables p', $\mathfrak{D}'$, B', and V' are defined in the same way in the $\{u,v\}$ space. $\mathfrak{D}$ must be assumed to be independent of both n and ε.

Within this notation, Eq. (13) reads

$$\frac{\partial c}{\partial t} = \vec{\nabla} \cdot BV = {}^t\vec{\nabla}BV + {}^tB\vec{\nabla} \cdot V = {}^t\nabla p\mathfrak{D}V + p\,{}^t\mathfrak{D}\vec{\nabla} \cdot V \tag{A1}$$

The problem is to find a system of coordinates $\{u,v\}$ in which the diffusion tensor $\mathfrak{D}'$ is the unit operator $\left(\begin{smallmatrix} 1 & 0 \\ 0 & 1 \end{smallmatrix}\right)$, so that the diffusion equation reads

$$\frac{\partial c'}{\partial t} = {}^t\vec{\nabla}'p'V' + p'\vec{\nabla}' \cdot V'. \tag{A2}$$

Let

$$\mathrm{Jac} = \begin{pmatrix} \partial n/\partial u & \partial n/\partial v \\ \partial \varepsilon/\partial u & \partial \varepsilon/\partial v \end{pmatrix}$$

be the Jacobian matrix of the $\{n,\varepsilon\} \to \{u,v\}$ transformation. The transformation is assumed to be linear, so that the elements of the Jacobian matrix are constants.

It can be shown that Eq. (A2) can be rewritten as

$$\frac{\partial c'}{\partial t} = {}^t({}^t\mathrm{Jac}\ \vec{\nabla})p'{}^t\mathrm{Jac}\ V + p'{}^t\mathrm{Jac}\ \vec{\nabla} \cdot {}^t\mathrm{Jac}\ V = {}^t\vec{\nabla}p'\mathrm{Jac}^t \cdot \mathrm{Jac}\ V + p'{}^t(\mathrm{Jac}^t \cdot \mathrm{Jac})\vec{\nabla} \cdot V \tag{A3}$$

The conditions for which Eq. (A3) is equivalent to Eq. (A1) are

$$\mathrm{Jac} \cdot {}^t\mathrm{Jac} = \mathfrak{D}, \tag{A4}$$

$$p' = p, \tag{A5}$$

$$c' = ac. \tag{A6}$$

Equation (A5) is satisfied just by replacing n and ε with their expressions as functions of u and v. It can be seen in Eq. (13) that c and c_0 can be multiplied by the same constant. This is also obviously true for c' and c_0', then a is an arbitrary constant.

One can arbitrarily suppose $\partial\varepsilon/\partial u = 0$, which allows further an easier interpretation by assuming a purely energetic dynamics along the v coordinate. The solution of Eq. (A4) is then

$$\frac{\partial n}{\partial u} = \frac{b}{\sqrt{b^2+q^2}},$$

$$\frac{\partial n}{\partial v} = \frac{b}{\sqrt{b^2+q^2}}\frac{q}{b},$$

$$\frac{\partial \varepsilon}{\partial v} = \frac{b}{\sqrt{b^2+q^2}}\frac{b^2+q^2}{b}.$$

The constant $b/\sqrt{b^2+q^2}$ can be removed from these three relations above and inserted in the constant a; then Feder's solution is exactly recovered as follows:

$$u = n - \frac{q}{b^2+q^2}\varepsilon, \tag{A7}$$

$$v = \frac{b}{b^2+q^2}\varepsilon. \tag{A8}$$

As stated above, the constant a can be chosen arbitrarily. Feder and co-workers chose the particular value $a = (b^2+q^2)/b$ in order to simplify the final calculation of the nucleation rate that involves the integral $\int_{-\infty}^{+\infty} c'dv$, which is equal in this case to $\int_{-\infty}^{+\infty} cd\varepsilon$. The nucleation dynamics and the final expression of the nucleation rate do not depend on this particular choice. Finally c_0' is given by

$$c_0'(u,v) = [(b^2+q^2)/b]c_0\left(u + \frac{q}{b}v, \frac{b^2+q^2}{b}v\right). \tag{A9}$$

The change of coordinate $\{n,\varepsilon\} \to \{u,v\}$ that diagonalizes the diffusion tensor is independent of any particular assumption on the equilibrium population c_0.

[1] J. Feder, K. C. Russell, J. Lothe, and G. M. Pound, Adv. Phys. **15**, 111 (1966).

[2] R. Becker and W. Döring, Ann. Phys. (Leipzig) **24**, 719 (1935).

[3] I. J. Ford, Phys. Rev. E **56**, 5615 (1997).

[4] D. W. Oxtoby, J. Phys.: Condens. Matter **4**, 7627 (1992).

[5] V. A. Shneidman, J. Chem. Phys. **115**, 8141 (2001).

[6] M. P. Anisimov, Russ. Chem. Rev. **72**, 591 (2003).

[7] P. Labastie and F. Calvo, in *Thermodynamics and Solid–Liquid Transition*, Nanomaterials and Nanochemistry, edited by C. Bréchignac, C. P. Houdy, and M. Lahmani (Springer, New York, 2007).

[8] J. Jortner, Z. Phys. D: At., Mol. Clusters **24**, 247 (1992).

[9] R. Bahadur and R. B. McClurg, J. Chem. Phys. **121**, 12499 (2004).

[10] J. Wölk, R. Strey, C. H. Heath, and B. E. Wyslouzil, J. Chem. Phys. **117**, 4954 (2002).

[11] Y. Viisanen, R. Strey, and H. Reiss, J. Chem. Phys. **99**, 4680 (1993).

[12] A. Dillmann and G. E. A. Meier, J. Chem. Phys. **94**, 3872

(1991).
[13] M. Blander and J. L. Katz, J. Stat. Phys. **4**, 55 (1972).
[14] R. B. McClurg and R. C. Flagan, J. Colloid Interface Sci. **201**, 194 (1998).
[15] D. Reguera and H. Reiss, Phys. Rev. Lett. **93**, 165701 (2004).
[16] S. L. Girshick and Chia-Pin Chiu, J. Chem. Phys. **93**, 1273 (1990).
[17] V. I. Kalikmanov, J. Chem. Phys. **124**, 124505 (2006).
[18] J. Belloni and P. Pernot, J. Phys. Chem. B **107**, 7299 (2003).
[19] J. C. Barrett, J. Chem. Phys. **116**, 8856 (2002).
[20] J. U. Andersen, E. Bonderup, K. Hansen, P. Hvelplund, B. Liu, U. V. Pedersen, and S. Tomita, Eur. Phys. J. D **24**, 191 (2003).
[21] J. C. Barrett and C. F. Clement, J. Aerosol Sci. **19**, 223 (1988).
[22] R. Strey, T. Schmeling, and P. E. Wagner, J. Chem. Phys. **85**, 6192 (1986).
[23] D. Brus, V. Ždímal, and F. Stratmann, J. Chem. Phys. **124**, 164306 (2006).
[24] J. Wedekind, A. P. Hyvärinen, D. Brus, and D. Reguera, Phys. Rev. Lett. **101**, 125703 (2008).
[25] J. Wedekind, D. Reguera, and R. Strey, J. Chem. Phys. **127**, 064501 (2007).
[26] V. M. Novikov, O. V. Vasil'ev, and H. Reiss, Phys. Rev. E **55**, 5743 (1997).
[27] J. Westergren, H. Grönbeck, S. G. Kim, and D. Tománek, J. Chem. Phys. **107**, 3071 (1997).
[28] J. Wölk and R. Strey, J. Phys. Chem. B **105**, 11683 (2001).
[29] J. Borggreen, F. Chandezon, O. Echt, H. Grimley, K. Hansen, P. M. Hansen, and C. Ristori, Eur. Phys. J. D **9**, 119 (1999).
[30] R. Kusche, Th. Hippler, M. Schmidt, B. Von Issendorf, and H. Haberland, Eur. Phys. J. D **9**, 1 (1999).
[31] A. Kantrowitz, J. Chem. Phys. **19**, 1097 (1951).
[32] R. F. Probstein, J. Chem. Phys. **19**, 619 (1951).
[33] R. McGraw and R. A. LaViolette, J. Chem. Phys. **102**, 8983 (1995).
[34] J. C. Barrett, C. F. Clement, and I. J. Ford, J. Phys. A **26**, 529 (1993).
[35] I. J. Ford and C. F. Clement, J. Phys. A **22**, 4007 (1989).
[36] B. E. Wyslouzil and J. H. Steinfeld, J. Chem. Phys. **97**, 2661 (1992).
[37] R. J. Anderson, R. C. Miller, J. L. Kassner, Jr., and D. E. Hagen, J. Atmos. Sci. **37**, 2508 (1980).
[38] D. Turnbull and J. C. Fisher, J. Chem. Phys. **17**, 71 (1949).
[39] L. S. Bartell, Annu. Rev. Phys. Chem. **49**, 43 (1998).
[40] I. J. Ford, J. Phys. Chem. B **105**, 11649 (2001).
[41] J. Hienola, M. Kulmala, and A. Laaksonen, J. Aerosol Sci. **32**, 351 (2001).
[42] J. Huang and L. S. Bartell, J. Phys. Chem. **99**, 3924 (1995).
[43] T. Koop, B. Luo, A. Tsias, and T. Peter, Nature (London) **406**, 611 (2000).
[44] M. Schmidt, R. Kusche, B. Von Issendorf, and H. Haberland, Nature (London) **393**, 238 (1998).
[45] G. A. Breaux, R. C. Benirschke, T. Sugai, B. S. Kinnear, and M. F. Jarrold, Phys. Rev. Lett. **91**, 215508 (2003).
[46] F. Chirot, P. Feiden, S. Zamith, P. Labastie, and J.-M. L'Hermite, J. Chem. Phys. **129**, 164514 (2008).
[47] T. P. Martin, U. Näher, H. Schaber, and U. Zimmermann, J. Chem. Phys. **100**, 2322 (1994).
[48] Ph. Buffat and J. P. Borel, Phys. Rev. A **13**, 2287 (1976).
[49] S. L. Lai, J. Y. Guo, V. Petrova, G. Ramanath, and L. H. Allen, Phys. Rev. Lett. **77**, 99 (1996).
[50] A. Bogdan, M. Kulmala, and N. Avramenko, Phys. Rev. Lett. **81**, 1042 (1998).
[51] J. Douady, F. Calvo, and F. Spiegelman, Eur. Phys. J. D **52**, 47 (2009).
[52] M. Schmidt, R. Kusche, T. Hippler, J. Donges, W. Kronmüller, B. von Issendorff, and H. Haberland, Phys. Rev. Lett. **86**, 1191 (2001).
[53] P. H. Chavanis, Int. J. Mod. Phys. B **20**, 3113 (2006).
[54] M. Bixon and J. Jortner, J. Chem. Phys. **91**, 1631 (1989).
[55] R. S. Berry and B. M. Smirnov, J. Chem. Phys. **114**, 6816 (2001).
[56] P. Labastie and R. L. Whetten, Phys. Rev. Lett. **65**, 1567 (1990).
[57] Y. Imry, Phys. Rev. B **21**, 2042 (1980).
[58] S. Zamith and J.-M. L'Hermite (unpublished).
[59] F. Chirot, P. Labastie, S. Zamith, and J.-M. L'Hermite, Phys. Rev. Lett. **99**, 193401 (2007).
[60] S. Zamith, P. Feiden, P. Labastie, and J-M. L'Hermite (unpublished).
[61] V. Weisskopf, Phys. Rev. **52**, 295 (1937).
[62] C. E. Klots, Z. Phys. D: At., Mol. Clusters **20**, 105 (1991).
[63] H. Reiss, P. Mirabel, and R. L. Whetten, J. Chem. Phys. **92**, 7241 (1988).
[64] J. Y. Tsao, M. J. Aziz, M. O. Thompson, and P. S. Peercy, Phys. Rev. Lett. **56**, 2712 (1986).
[65] M. Y. Hahn and R. L. Whetten, Phys. Rev. Lett. **61**, 1190 (1988).
[66] R. S. Berry and D. J. Wales, Phys. Rev. Lett. **63**, 1156 (1989).
[67] H. A. Kramers, Physica VII **4**, 284 (1940).
[68] N. Destainville, Soft Matter **4**, 1288 (2008).
[69] B. Chen, J. I. Siepmann, and M. L. Klein, J. Phys. Chem. A **109**, 1137 (2005).